



**HAL**  
open science

# Hydrates and polymorphs of lead squarate $\text{Pb}(\text{C}_4\text{O}_4)$ : Structural transformations studied by in situ X-ray powder diffraction and solid state NMR

Thierry Bataille, A. Bouhali, Cassandre Kouvatas, C. Trifa, Nathalie  
Audebrand, C. Boudaren

## ► To cite this version:

Thierry Bataille, A. Bouhali, Cassandre Kouvatas, C. Trifa, Nathalie Audebrand, et al.. Hydrates and polymorphs of lead squarate  $\text{Pb}(\text{C}_4\text{O}_4)$ : Structural transformations studied by in situ X-ray powder diffraction and solid state NMR. *Polyhedron*, 2019, 164, pp.123-131. 10.1016/j.poly.2019.02.047 . hal-02090016

**HAL Id: hal-02090016**

**<https://univ-rennes.hal.science/hal-02090016>**

Submitted on 6 Jun 2019

**HAL** is a multi-disciplinary open access archive for the deposit and dissemination of scientific research documents, whether they are published or not. The documents may come from teaching and research institutions in France or abroad, or from public or private research centers.

L'archive ouverte pluridisciplinaire **HAL**, est destinée au dépôt et à la diffusion de documents scientifiques de niveau recherche, publiés ou non, émanant des établissements d'enseignement et de recherche français ou étrangers, des laboratoires publics ou privés.

# Hydrates and polymorphs of lead squarate $\text{Pb}(\text{C}_4\text{O}_4)$ : structural transformations studied by *in situ* X-ray powder diffraction and solid state NMR

Thierry Bataille<sup>\*,a</sup>, Amira Bouhali,<sup>b</sup> Cassandre Kouvatat,<sup>a,c</sup> Chahrazed Trifa,<sup>b</sup> Nathalie Audebrand,<sup>a</sup> Chaouki Boudaren<sup>b</sup>

<sup>a</sup> Univ Rennes, Ecole Nationale Supérieure de Chimie de Rennes, CNRS, ISCR - UMR 6226, F- 35000 Rennes, France

<sup>b</sup> Unité de Recherche de Chimie de l'Environnement et Moléculaire Structurale CHEMS, Université Mentouri de Constantine, route de Ain El-Bey, 25017 Constantine, Algeria

<sup>c</sup> Laboratoire Catalyse et Spectrochimie, Normandie Univ, ENSICAEN, UNICAEN, CNRS, 6 Marechal Juin, 14050 Caen, France

## Abstract

Considering the low dimensionality of the crystal structure of the known lead squarate tetrahydrate,  $\text{Pb}(\text{C}_4\text{O}_4)\cdot 4\text{H}_2\text{O}$ , the thermal reactivity of the powdered compound and structural studies of lower hydrates have been investigated from X-ray single-crystal and powder diffraction data, solid state NMR and thermal analyses. It is shown that  $\text{Pb}(\text{H}_2\text{O})(\text{C}_4\text{O}_4)$  and two polymorphs of anhydrous  $\text{PbC}_4\text{O}_4$  can be formed within different conditions. Crystal data of the new phases are:  $\text{Pb}(\text{H}_2\text{O})(\text{C}_4\text{O}_4)$  (**1**), S.G.  $P2_1/c$ ,  $a = 7.3650(5)$  Å,  $b = 11.302(1)$  Å,  $c = 6.6822(4)$  Å,  $\beta = 102.501(6)^\circ$ ,  $Z = 4$ ;  $\text{PbC}_4\text{O}_4$  (**2**), orthorhombic crystal system,  $a = 24.276(6)$  Å,  $b = 15.261(3)$  Å,  $c = 7.850(2)$  Å,  $Z = 4$ ;  $\text{PbC}_4\text{O}_4$  (**3**), S.G.  $I4/mcm$ ,  $a = 6.1640(2)$  Å,  $c = 12.0526(8)$  Å,  $Z = 4$ . The departure of the water molecules leads to the condensation of initial inorganic chains into 2D or 3D-type crystal structures. The full decomposition of the squarate ligand provides successive lead oxides.

**Keywords:** lead squarate, in situ powder diffraction, solid state NMR, thermal behaviour, phase transformation and polymorphism

## 1. Introduction

Oxocarbon 3,4-dihydroxy-3-cyclo-butene-1,2-dione (squaric acid,  $\text{H}_2\text{C}_4\text{O}_4$ ), first synthesized by Cohen, Lacher & Park [1], is of wide interest because of its cyclic structure, and the possible aromaticity and the variety of coordination modes of its bases [2] West & Niu [3] described the preparation from aqueous solutions of ‘isostructural’ divalent metal squarates of general formula  $\text{MC}_4\text{O}_4 \cdot 2\text{H}_2\text{O}$  ( $M = \text{Ca, Mn, Fe, Co, Ni, Cu, Zn}$ ), and predicted a chelated linear polymer structure later disclaimed by Habenschuss & Gerstein [4], who showed that  $\text{Ni}(\text{C}_4\text{O}_4) \cdot 2\text{H}_2\text{O}$  has a 3-dimensional structure. A few structures have been published for the other isostructural transition-metal squarates ( $\text{Cu, Co}$ ) [5,6]. Furthermore, it has been shown in the past that the squarate ligand could connect metal atoms in a bidentate fashion as the oxalate group. [7,8]. In the structurally well understood metal squarates  $M(\text{C}_4\text{O}_4)(\text{H}_2\text{O})_4$  ( $M = \text{Mn, Fe, Co, Ni, Zn}$ ), [9] the  $\text{C}_4\text{O}_4^{2-}$  entity serves as a bridging ligand between two metal ions ( $\mu$ -2) in *trans* positions while it acts as a fourfold monodentate ( $\mu$ -4) ligand between metals in the three-dimensional polymeric structures of  $M(\text{C}_4\text{O}_4)(\text{H}_2\text{O})_2$  ( $M = \text{Mn, Fe, Co, Ni, Cu, Zn}$ ), in the layered cobalt oxalate-squarate  $\text{Co}_2(\text{C}_4\text{O}_4)(\text{C}_2\text{O}_4)(\text{C}_3\text{N}_2\text{H}_2)_2$  [10] and in tin(II) squarate  $\text{Sn}_2\text{O}(\text{C}_4\text{O}_4)(\text{H}_2\text{O})$ . [11]

On the other hand,  $\text{Pb}^{\text{II}}$  compounds have been increasingly studied, owing to the toxicity of lead in environment and in biological systems and for the specific interactions of lead through its sterically active  $6s^2$  lone electron pair. Usually, eightfold coordination number around Pb cations is the most commonly found. [12-14] In lead squarate tetrahydrate,  $\text{Pb}(\text{H}_2\text{O})_4(\text{C}_4\text{O}_4)$ , [15] the coordination polyhedron of Pb is described as mono face-capped and edge-capped trigonal prisms, while with a symmetric electron shell Ba cation in  $\text{BaC}_4\text{O}_4$ , [16] the Ba polyhedron is a distorted square antiprism, where the ligand acts as a  $\mu_8$  connector.

The present study deals with the formation of three new lead squarates,  $\text{Pb}(\text{H}_2\text{O})(\text{C}_4\text{O}_4)$  (**1**) and two  $\text{PbC}_4\text{O}_4$  polymorphs (**2**), (**3**). Compounds (**1**) and (**2**) were obtained from the thermal dehydration of lead (II) squarate tetrahydrate  $\text{Pb}(\text{H}_2\text{O})_4(\text{C}_4\text{O}_4)$  [15], while the second  $\text{PbC}_4\text{O}_4$  polymorph (**3**) was hydrothermally prepared. Their structural relationships are discussed and compared to the known precursor, as well as to other metal squarates, in terms of topologies and Pb coordination modes.

## 2. Experimental section

### 2.1. Materials

All chemicals were commercially available and used as received. For convenience, 3,4-dihydroxy-3-cyclo-butene-1,2-dione ( $\text{H}_2\text{C}_4\text{O}_4$ , Acros Organic 99%) is named squaric acid hereafter. The other reagent is  $\text{Pb}(\text{NO}_3)_2$  (rectapur >98.5%) from Prolabo.

### 2.2. Aqueous syntheses of $\text{Pb}(\text{H}_2\text{O})_4(\text{C}_4\text{O}_4)$ precursor and $\text{PbC}_4\text{O}_4$ (**3**)

The white fine powder of  $\text{Pb}(\text{H}_2\text{O})_4(\text{C}_4\text{O}_4)$  was obtained by precipitation of lead cations by a squaric acid solution. The conditions to obtain a single phase material were as follows: lead nitrate  $\text{Pb}(\text{NO}_3)_2$  (1.5 mmol) was dissolved at room temperature in 20 mL of distilled water. This solution was slowly titrated under constant stirring by 0.1M squaric acid solution, added in a small excess to ensure the complete precipitation. The precipitate was filtered off, washed with distilled water, and dried at room temperature.

$\text{PbC}_4\text{O}_4$  (**3**) was synthesized under hydrothermal conditions, starting from a mixture of lead nitrate  $\text{Pb}(\text{NO}_3)_2$ , squaric acid  $\text{H}_2\text{C}_4\text{O}_4$  and distilled water in the molar ratio 1/4/370. The suspension was stirred for 20 minutes until homogenised. The final mixture was sealed in a 23 mL Teflon-lined acid digestion bomb (Parr) and heated at 180 °C for 28 h under autogeneous pressure and then cooled down to room temperature. The white crystalline product obtained as small polygonal crystals was collected by filtration, thoroughly washed with distilled water and ethanol, and finally dried at room temperature.

### 2.3. Solid state synthesis of $\text{Pb}(\text{H}_2\text{O})(\text{C}_4\text{O}_4)$ (**1**).

The pristine phase  $\text{Pb}(\text{H}_2\text{O})_4(\text{C}_4\text{O}_4)$  was heated at 40 °C overnight to form the desired compound (**1**). A tiny amount of phase (**3**) was detected in the sample. Heating the precursor at lower temperature could not lead to the full removal of the expected 3 water molecules.

### 2.4. Thermal analyses

Temperature-dependent powder X-ray diffraction (TDXD) (Fig.1) was performed with a powder diffractometer combining the curved-position-sensitive detector from INEL (CPS 120) and a high-temperature attachment from Rigaku. The detector was used in a semi-focusing arrangement by reflection ( $\text{CuK}\alpha_1$  radiation) as described elsewhere. [17] An angle of 6° was selected between the incident beam and the surface of the sample. The

decomposition was carried out, under flowing air, with a heating rate of  $10\text{ }^{\circ}\text{C h}^{-1}$  from room temperature to  $600\text{ }^{\circ}\text{C}$ . To ensure satisfactory counting statistics, a counting time of 1800 s per pattern was selected for the thermal decomposition of the precursor. Temperature calibration is usually carried out with standard materials in the given temperature range. *In situ* X-ray powder diffraction patterns were also collected at various temperatures with the Bruker AXS D5005 diffractometer described below. Thermogravimetric analysis (TG) (Fig.2) was carried out with a Rigaku Thermoflex instrument under airflow with a heating rate of  $10\text{ }^{\circ}\text{C h}^{-1}$ . The powdered sample was spread evenly in a large platinum crucible to avoid mass effects.

### 2.5. X-ray powder diffraction data collection and structure determination

*Lead squarate monohydrate*  $\text{Pb}(\text{H}_2\text{O})(\text{C}_4\text{O}_4)$  (**1**). Laboratory powder data were obtained with a Siemens D500 diffractometer using monochromatic  $\text{Cu K}\alpha_1$  radiation ( $\lambda = 1.5406\text{ \AA}$ ) selected with an incident beam curved-crystal germanium monochromator, using the parafocusing Bragg–Brentano geometry. The pattern was scanned at room temperature, over the angular range  $10\text{--}130^{\circ}$  ( $2\theta$ ), with a step length of  $0.02^{\circ}$  ( $2\theta$ ) and a counting time of  $40\text{ s step}^{-1}$ . For pattern indexing, the extraction of peak positions was carried out with the Socabim fitting program available in the PC software package *DiffraC<sup>plus</sup>* supplied by Bruker AXS. Powder pattern indexing was performed with the program DICVOL04. [18] From the first 20 lines of the X-ray powder diffraction pattern selected for pattern indexing, 17 lines were indexed on the basis of a monoclinic solution with an absolute error of  $0.03^{\circ}$  ( $2\theta$ ) on the peak positions, the remaining 3 diffraction lines being considered as spurious reflections by the software. A least-squares refinement from the first 36 resolved diffraction lines available led to the unit cell dimensions  $a = 7.366(1)\text{ \AA}$ ,  $b = 11.305(2)\text{ \AA}$ ,  $c = 6.685(1)\text{ \AA}$ ,  $\beta = 102.49(1)^{\circ}$  and  $V = 543.4\text{ \AA}^3$  [ $M_{20} = 86$ ;  $F_{30} = 150(0.005, 39)$ ]. The systematic absences revealed by a careful examination of the powder data are consistent with the space group  $P2_1/c$  (No. 14). The non-indexed peaks were identified as those of one anhydrous lead squarate  $\text{PbC}_4\text{O}_4$  (**3**) described below. Structure determination was carried out using the parallel tempering algorithm available in the global optimization program FOX. [19] Calculations were performed on a personal computer, starting from one each of Pb,  $\text{C}_4\text{O}_4$  and  $\text{H}_2\text{O}$  groups. The solution was found after 20 million trials. Structure refinement was achieved with the program FULLPROF within the FullProf suite [20]. A pseudo-Voigt function was used to describe the individual line profiles and the usual quadratic Caglioti function in  $\tan\theta$  was

selected to characterize the angular dependence of peak widths. The background was described with a linear interpolation between twelve refined intensity points. Pb displacement parameters were refined in anisotropic manner. Profile and structural parameters of  $\text{PbC}_4\text{O}_4$  (**3**) described below were also refined as a second phase. Crystallographic data and details of the Rietveld refinements are given in Table 1. The final Rietveld plot for  $\text{Pb}(\text{H}_2\text{O})(\text{C}_4\text{O}_4)$  (Fig. 3) shows good agreement between experimental and calculated patterns. Final atomic coordinates and isotropic atomic displacement parameters are displayed in Table 2 and selected distances are listed in Table 3. The program DIAMOND (version 3.2h), supplied by Crystal Impact, was used for structure drawings.

*Lead squarate polymorph  $\text{PbC}_4\text{O}_4$  (2).* Starting from  $\text{Pb}(\text{H}_2\text{O})_4(\text{C}_4\text{O}_4)$ , powder data of (**2**) were collected in air at 140 °C with a Bruker AXS D5005 diffractometer using a diffracted-beam-graphite monochromator ( $\text{CuK}\alpha_{1,2}$ ) and equipped with a Anton Paar HTK1200 oven camera. The pattern was scanned over the angular range 5.00 – 120.00° ( $2\theta$ ), step size 0.02° ( $2\theta$ ), step time 70 s step<sup>-1</sup> (Fig. S1). Powder pattern indexing was performed with the program DICVOL04 on the basis of available diffraction lines whose positions were extracted with *DiffraC<sup>plus</sup>*, leading to the orthorhombic unit cell  $a = 24.268(4)$  Å,  $b = 15.270(3)$  Å,  $c = 7.854(1)$  Å, and  $V = 2910.6$  Å<sup>3</sup> [ $M_{20} = 26$ ,  $F_{25} = 48(0.0053, 98)$ ]. Examination of the systematic absences from the whole available diffraction lines enabled to determine unambiguously the presence of a glide plane associated with the absence of  $0\ k\ l$ ,  $k = 2n+1$  reflections. However, the line overlap due to the relatively large unit cell, combined with the presence of diffraction peaks from the other polymorph (**3**), did not allow to ensure the extinction conditions for either the crystal lattice or the symmetry operations. The possible conditions for extinction were then  $hkl$ ,  $l = 2n+1$ ;  $0kl$ ,  $k = 2n+1$ ;  $h0l$ ,  $h = 2n+1$ ;  $h00$ ,  $h = 2n+1$  and  $0k0$ ,  $k = 2n+1$ .

Any space groups that agree the extinction conditions were sampled, from the less to the most symmetric one, i.e. from *Pmnm* to *Cmma* (in agreement with permutation of unit cell parameters if required). Heavy Pb atoms were tried to be located from Patterson method, direct methods and Monte Carlo – parallel tempering calculations, using complete structural models (i.e., including squarate groups) in the last case. All models proposed Pb atoms placed at the same positions. It was then deduced, from the expected maximum number of atoms per unit cell (~170 on the assumption that the volume of a non H-atom is ~17 Å<sup>3</sup>) and the special positions of the studied space groups that the most probable space group was *Cmma*. Even

starting with these positions (given in Table 2), no squarate groups could be undoubtedly placed. In order to complete the partial structure model given here, hydrothermal syntheses of  $\text{PbC}_4\text{O}_4$  were performed at high temperatures (up to 180 °C). Unfortunately, only polymorph (3) of lead squarate could be obtained as a pure phase.

*Single-crystal diffraction data collection of  $\text{PbC}_4\text{O}_4$  (3).* A suitable single crystal of linear dimensions  $0.1 \times 0.08 \times 0.08$  mm was carefully selected. Intensity data were collected on a four-circle Nonius Kappa CCD diffractometer equipped with a CCD area detector, using the  $\text{MoK}\alpha$  radiation ( $\lambda=0.71073$  Å) operating at 55kV and 28 mA. Intensity data sets were collected at room temperature by using the program COLLECT [21] available in the Kappa CCD software package. Lorentz-polarization factor correction, peak integration and background determination were carried out with the program DENZO. Frame scaling and unit-cell parameters refinement were made with the program SCALEPACK. [22] Analytical absorption corrections were performed by modeling the crystal faces. [23] The crystal structure was solved in the tetragonal symmetry, space group  $I4/mcm$ . The complete model was found using the direct methods with the program SIR2002 [24] and refined by SHELXL-97. [25] The final atomic coordinates together with their equivalent isotropic displacement parameters are listed in Table 2. Selected bond distances are reported in Table 3.

### 2.6. Solid-state NMR

$^1\text{H}$  and  $^{207}\text{Pb}$  solid-state NMR experiments were performed using a Bruker Avance III spectrometer equipped with a 11.7 T magnet and a 4 mm probehead at Larmor frequencies of 500.13 and 104.63 MHz for  $^1\text{H}$  and  $^{207}\text{Pb}$ , respectively. Experiments were carried out using RF field strengths of  $\nu_1^{\text{H}} = 71.4$  kHz and  $\nu_1^{\text{Pb}} = 45.5$  kHz, and MAS rates of 14 kHz and 13.3 kHz for  $^1\text{H}$  and  $^{207}\text{Pb}$  respectively. Recycle delays were set to 5 s for  $^1\text{H}$  and 10 s for  $^{207}\text{Pb}$ .  $^1\text{H}$  and  $^{207}\text{Pb}$  spectra were referenced using adamantane and solid  $\text{Pb}(\text{NO}_3)_2$  as a secondary external reference, relatively to tetramethyllead (TML) at 298 K. The isotropic chemical shifts of lead spectra were carefully corrected by taking into account the increase of the sample temperature due to the spinning. [26] Several spinning rates were tested to identify the isotropic signals. Spectra treatment was performed using DMFIT software, considering all spinning sideband manifold. [27]

### 3. Results and discussion

#### 3.1. Thermal behaviour of $Pb(H_2O)_4(C_4O_4)$

*Dehydration of the precursor.* The TDXD plot (Fig. 1) shows that the dehydration of the precursor proceeds in two stages. At the lowest temperatures (20-40 °C), powder patterns agree with the presence of  $Pb(H_2O)(C_4O_4)$  (**1**) together with a small amount of the tetrahydrate precursor. A further *ex situ* experiment revealed that  $Pb(H_2O)_4(C_4O_4)$  slowly dehydrates into the monohydrated phase after being milled for homogeneity, which explains the presence of both compounds at room temperature in the TDXD plot. This is confirmed by the TG analysis (Fig. 2) performed with an aged ground powder, which demonstrates that the tetrahydrate precursor did no longer exist at the beginning of the experiment. Both TG curve and TDXD plot show that  $Pb(H_2O)(C_4O_4)$  (**1**) dehydrates at 110 °C (weight loss: exp. 5.5 %; theor. 5.3 %). Powder patterns of a compound with the given formula  $PbC_4O_4$  are thus observed between 120 and 285 °C in Fig. 1. A thorough search for similar patterns was performed within the ICDD (International Centre for Diffraction Data) PDF2 database [28] without success. Then, it was of interest to solve the crystal structure of this anhydrous compound, which appears as a new polymorph of anhydrous lead squarate, identified as (**2**) hereafter.

*Formation of  $PbC_4O_4$  polymorphs.* Powder patterns of  $PbC_4O_4$  (**2**), as identified on the TDXD plot between 120 °C and 285 °C, could be obtained between 120 and 150 °C by heating powder samples of fresh  $Pb(H_2O)_4(C_4O_4)$  placed on a nickel grid into a high-temperature camera attached to a diffractometer ( $CuK\alpha_{1,2}$ ). For any patterns in this temperature range, it was observed that three phases could exist together (Fig. 4). Fast heating regimes (ca. 30 °C h<sup>-1</sup>) favours the full dehydration into  $PbC_4O_4$ , but the unknown anhydrous polymorph (**2**) is accompanied with a high amount of  $PbC_4O_4$  (**3**), as demonstrated by the presence of some more intense diffraction lines corresponding to its calculated powder pattern (Figure 4c). With slower heating regimes (< 10 °C h<sup>-1</sup>),  $PbC_4O_4$  (**2**) was formed quantitatively and the amount of polymorph (**3**) could be decreased significantly but not fully removed, while  $Pb(H_2O)(C_4O_4)$  (**1**) remained as a minor phase (Fig. 4d). The best compromise to collect data of (**2**) was actually to heat a monohydrate sample at a rate of 28.8 °C h<sup>-1</sup> up to 140 °C, in order to remove diffraction lines of  $Pb(H_2O)(C_4O_4)$  (**1**). As explained above,  $PbC_4O_4$

polymorph **(3)** is also readily obtained by the dehydration of lead squarate tetrahydrate at lower temperatures (between RT and 40 °C), as it was observed as impurity in the powder pattern of  $\text{Pb}(\text{H}_2\text{O})(\text{C}_4\text{O}_4)$ . It was then concluded that  $\text{PbC}_4\text{O}_4$  **(2)** is the most thermodynamically stable polymorph obtained from a gentle dehydration, while  $\text{PbC}_4\text{O}_4$  polymorph **(3)** is kinetically favoured upon dehydration.

*Thermal decomposition of  $\text{PbC}_4\text{O}_4$  into lead oxides.* Fig. 1 (TDXD) and Fig. 2 (TGA) show that further heating of  $\text{PbC}_4\text{O}_4$  above 285 °C leads to the decomposition of the squarate group into successive lead oxides. The first badly crystallised phase (285-305 °C) observed on the TDXD plot could not be clearly identified, but comparison of its powder pattern to those of lead-containing carbonates suggests that  $\text{Pb}_2\text{OCO}_3$  (ICDD PDF 00-48-1888) is formed before the apparition of  $\alpha$ -PbO (litharge, ICDD PDF 03-65-0400), observed in the short temperature range of 305-330 °C (weight loss: exp. 35.1 %; theor. 34.8 %). This last phase is not stable at this temperature [29] and oxidises rapidly into  $\text{Pb}_2\text{O}_3$  (ICDD PDF 01-76-1832), observed between 330 °C and 460 °C. It is consistent with the slow increase of the sample mass seen on the TG curve carried out under airflow (weight loss: exp. 33.3 %; theor. 31.9 %). As described previously, [30]  $\text{Pb}_2\text{O}_3$  reduces at higher temperature, to form  $\text{Pb}_3\text{O}_4$  seen on the TDXD plot in the range 460-575 °C (weight loss: exp. 34.3 %; theor. 32.8 %). The last reduction stage is finally observed at 575 °C, where  $\alpha$ -PbO is formed again. A such oxidation-reduction mechanism of  $\alpha$ -PbO has been well described, in particular after decomposition of lead carboxylates. [29,31]

### 3.2. Crystal structures of lead squarates

*$\text{Pb}(\text{H}_2\text{O})(\text{C}_4\text{O}_4)$  **(1)**.* The crystal structure of **(1)** consists in one Pb, one water molecule and one squarate anion in the asymmetric unit, connected together to form a three-dimensional framework. The lead cation is eight-fold coordinated in a quite regular dodecahedral fashion by two water molecules, four O atoms from four monodentate squarate groups and two O atoms from one squarate engaged in a chelating mode (Fig. 5a). The Pb-O distances fall in the range 2.56(1)-2.88(1) Å, the longest bond arising from Ow. They are in agreement with Pb-O distances observed in other  $\text{Pb}^{\text{II}}$  complexes. [15,32,33] The squarate anion acts as a bridging ligand with a tetra(monodentate) and a chelate coordination mode ( $\mu_6$ ) to five Pb cations. Pb polyhedra share two edges through either two water O atoms or two O1 atoms, to form zig-

zag chains running along the  $a$  axis. The connexion between adjacent chains is ensured by corner-shared  $\text{PbO}_8$  dodecahedra through squarate oxygen atoms. The inorganic linkage, created by Pb-O bonds, forms a dense packing with small 6-membered rings apertures into which are located the squarate groups (Fig. 5b).

The crystal symmetry determined from an X-ray experiment is representative of the combination of the symmetry operators over the 3-D crystal space. On the contrary, NMR is a probe of the local symmetry of some observed nuclei, as for example proton  $^1\text{H}$ . In the structure of **(1)**, the water molecule is represented only by its oxygen atom  $\text{O}_w$ , as electron density of H atoms cannot be determined easily from X-ray powder data.  $\text{O}_w$  is bonded to two Pb atoms with the distances of 2.58(1) Å and 2.88(1) Å. Possible hydrogen bonds can be formed between  $\text{O}_w$  and  $\text{O}_3$  (2.73 Å) and  $\text{O}_4$  (2.61 Å) according to the pseudo-tetrahedral geometry of a water molecule. A  $^1\text{H}$  NMR experiment would be helpful in looking insight into the geometry of the water molecule, due to its sensibility to the variation of local environments of probed protons.

The  $^1\text{H}$  MAS NMR spectrum of  $\text{Pb}(\text{H}_2\text{O})(\text{C}_4\text{O}_4)$  **(1)** (Fig. 6a and Fig. S2) shows four isotropic signals at 1.75, 4.56, 6.53, and 9.10 ppm, with integrated intensities of 8%, 22%, 37% and 33% respectively for signals denoted as  $\text{H}_1$ ,  $\text{H}_2$ ,  $\text{H}_3$  and  $\text{H}_4$  on the spectrum.

The crystal symmetry of **(1)**, leading to the undoubtedly determined space group  $\text{P}2_1/\text{c}$ , must involve two symmetry-inequivalent water H atoms in term of Wyckoff positions. At first sight, the  $^1\text{H}$  MAS NMR experiment would suggest four inequivalent H atoms in the structure, which is, in the symmetry point of view, inadequate with the given symmetry. Actually, if the actual symmetry was broken, one would expect two well distinct signals from a  $^{207}\text{Pb}$  NMR experiment with a significant chemical shift difference, as described by Fayon et al. [34].

A  $^{207}\text{Pb}$  NMR spectrum was measured and presented in Fig. 6b and Fig. S3. Two isotropic signals appear at -2401 and -2417 ppm (with integrated intensities of 30% and 70% respectively), which are more visible in the spinning sideband manifold. It is assumed that the chemical shift is dependent on the Pb-O distances [34]. In the present spectrum, the two isotropic signals are separated by 16 ppm only, which corresponds to a Pb-O length difference of 0.0018 Å. Such difference is negligible regarding the X-ray diffraction analysis, as it belongs to the uncertainty of any Pb-O bond (see Table 3) and of the ellipsoidal Pb displacement parameters. In the average structure of **(1)**, one can consider that there is only one Wyckoff position for Pb, as given by the actual space group  $\text{P}2_1/\text{c}$ . However, the  $^{207}\text{Pb}$  NMR experiment demonstrates that there are small local variations in the environment of Pb,

which may be linked to the  $^1\text{H}$  MAS NMR experiment results. Indeed, the intensity of the signal denoted  $\text{Pb}_1$  in Fig. 6b is equal to the sum of the intensities of the two signals denoted  $\text{H}_1$  and  $\text{H}_2$  in Fig. 6a, i.e. 30 %. In the same manner, the intensity of signal  $\text{Pb}_2$  and the sum of signals  $\text{H}_3$  and  $\text{H}_4$  is 70 %. In addition, the  $\text{Pb}_1$ ,  $\text{H}_1$  and  $\text{H}_2$  signals are the lesser shifted, while the  $\text{Pb}_2$ ,  $\text{H}_3$ ,  $\text{H}_4$  signals are the most shifted from the origin in their relative spectra. The Pb and the H atoms actually delineate the tetrahedral geometry around the water oxygen  $\text{O}_w$  atom. The tetrahedron is easy to depict with the acceptor O atoms instead of water H atoms that are not localised from XRD data (Fig. S4). It is clear that each oxygen atom is involved in two sets of Pb-O distances, leading to four distinct Pb-O distances forming the edges of the tetrahedron. In a hydrogen bond, H belongs to the vicinity of  $\text{O}_w$  in the direction of the O acceptor atom. Thus, the same reasoning applies, i.e., there is four distinct Pb-H distances as well around the central  $\text{O}_w$  atom, leading to four  $^1\text{H}$  atom environments as suggested in the NMR spectrum (Fig. 6a).

*PbC<sub>4</sub>O<sub>4</sub> (2)*. Although powder data could not allow locating organic moieties, the positions of lead atoms give partial information of the structure arrangement of this polymorph. Fig. 7 shows the dense framework of Pb atoms within the unit cell. Within such heavy atom arrangement, raw Pb-Pb distances range from 4.02 Å to 4.54 Å, as discussed below. All but the shortest are typical distances observed in other squarate phases reported here, and more generally in lead carboxylates. [35,36].

*PbC<sub>4</sub>O<sub>4</sub> (3)*. Fig. 8 shows that the 3-dimensional structure of the compound exhibits a strong 2D character. It is built from inorganic layers of edge-sharing  $\text{PbO}_8$  square antiprisms, pillared by the squarate groups along the c axis. Each Pb atom is connected through oxygen to eight squarate entities, the last acting as  $\mu_8$  monodentate anions. The compound is actually isostructural with  $\text{BaC}_4\text{O}_4$  [16] (space group *I4/mcm*) and with  $\text{YKC}_4\text{O}_4$  [37] (space group *P4/mcc*). It is not surprising as ionic radii of 8-coordinated cations (or mixed cations) in the three compounds are comparable, i.e., 1.56 Å for  $\text{Ba}^{2+}$ , 1.43 Å for  $\text{Pb}^{2+}$ , and 1.41 Å for mixed  $\text{Y}^{3+}/\text{K}^+$ . The crystal structure of  $\text{Cd}_2(\text{C}_4\text{O}_4)(\text{OH})_2$  [38] also possesses a similar 2D behaviour, in which the squarate anions connect the inorganic layers as a manner of oblique pillars. However the ionic radius of  $\text{Cd}^{2+}$  is 1.09 Å in its octahedral environment, made up from not only squarates but two  $\text{OH}^-$ , which favours layered structures such as Layered Double Hydroxides. [39] Interestingly, while the squarate anion adopts a  $\mu_8$  coordination mode in  $\text{AgC}_4\text{O}_4$  [40] that should suggest a similar structural feature, its crystal structure built from 5-

and 6-fold coordinated  $\text{Ag}^+$  belongs to another topology, related to the ionic radius of silver in a 6-coordination mode of 1.29 Å.

### 3.3. Evolution of the structures upon dehydration.

Fig. 9 shows the modifications of the lead atom environment as water molecules release from  $\text{Pb}(\text{H}_2\text{O})_4(\text{C}_4\text{O}_4)$  to  $\text{PbC}_4\text{O}_4$  (**3**). The inorganic part, symbolised by linkages between Pb atoms, is schemed together with the squarate anions, to show the topologies of the structure models.

In  $\text{Pb}(\text{H}_2\text{O})_4(\text{C}_4\text{O}_4)$ , Pb is 8-fold coordinated to two monodentate and one chelating squarates, and four water molecules. The departure of three of the four water molecules leads to the bonding of two more monodentate squarate groups in  $\text{Pb}(\text{H}_2\text{O})(\text{C}_4\text{O}_4)$  (**1**), while the remaining  $\text{H}_2\text{O}$  is twice connected to Pb by symmetry. While the structure of the tetrahydrate precursor could be described as inorganic  $[\text{PbO}_2]_n$  chains connected together by both water and organic ligands (Fig. 9a), the dehydration process gives rise to the condensation of these chains into the three-dimensional inorganic framework of (**1**) (Fig. 9b). Considering Pb-Pb distances, lead atoms are separated by 4.43 Å through edge-shared polyhedra in the tetrahydrate precursor. In (**1**), the edge-sharing within the chains is preserved, providing usual Pb-Pb distances of 4.41 and 4.52 Å. The linkage between chains is ensured by corner-shared Pb polyhedra, with a longer distance of 4.91 Å, as depicted by dashed lines in Fig. 9b. The release of the last water molecule leads to  $\text{PbC}_4\text{O}_4$ , either (**2**) or (**3**). In (**3**), a significant structural rearrangement occurs, as the inorganic part is clearly 2-dimensional (Fig. 9c), in which Pb atoms are connected through edge-shared polyhedra only, with a typical Pb-Pb distance of 4.36 Å. In the anhydrous compound (**2**), all Pb atoms are separated by distances between 4.34 and 4.54 Å, except one Pb2-Pb2 distance of 4.02 Å. While its crystal structure model is partial, it is however expected that Pb atoms involved in the first set of distance share their polyhedra in a edge-shared fashion, with regard to the previous lead squarate. Though the Pb2-Pb2 distance is very short with regard to the others, this value can be readily compared with these observed in  $\text{PbSeO}_3$  [41] or  $\text{PbCrO}_3$  [42]. Such typical Pb-Pb distance of ca 4.0 Å is the result of face-sharing Pb polyhedra through three oxygen atoms, which is also assumed in (**3**). Thus, the two expected connexion modes in three non-collinear directions clearly lead to a 3-dimensional inorganic framework of (**2**) (Fig. 9d).

## 4. Conclusion

Lead squarate tetrahydrate  $\text{Pb}(\text{H}_2\text{O})_4(\text{C}_4\text{O}_4)$ , an ordinary compound whose crystal structure has been described for a couple of years,<sup>13</sup> has revealed an astonishing reactivity when subjected to grinding and temperature exposure. The study of its thermal behaviour from coupled *in situ* X-ray powder diffraction, solid state NMR and thermogravimetric analysis has enabled to identify a new monohydrate phase and two polymorphs of its anhydrous state. The transformations between each phase could be described in term of stability with regard to the sample environment, which allowed the preparation of one  $\text{PbC}_4\text{O}_4$  polymorph in a single-crystal form. The crystal structures of the observed phases, solved from either single-crystal or powder data – at least partly for the second  $\text{PbC}_4\text{O}_4$  polymorph – could provide fruitful information to give a detailed description of the structural rearrangements that occur upon dehydration. This study is one of a series of our investigations of simple hydrated compounds from *in situ* XRPD, which bring to light the structural diversity of non-ambient metastable and stable phases.

## Appendix A. Supplementary data

CCDC 915400 contains the supplementary crystallographic data for **(3)**. These data can be obtained free of charge via <http://www.ccdc.cam.ac.uk/conts/retrieving.html>, or from the Cambridge Crystallographic Data Centre, 12 Union Road, Cambridge CB2 1EZ, UK; fax: (+44) 1223-336-033; or e-mail: [deposit@ccdc.cam.ac.uk](mailto:deposit@ccdc.cam.ac.uk).

Supplementary data to this article are available online.

## Acknowledgements

The authors thank Dr Thierry Roisnel (<http://www.cdifx.univ-rennes1.fr>) for assistance in X-ray single-crystal data collection. FEDER contributed to the purchase of the AVIII 500 MHz solid state NMR spectrometer at the LCS.

## References

- [1] S. Cohen, J. R. Lacher and J. D. Park, *J. Am. Chem. Soc.* 81(1959) 3480.

- [2] B. Zheng, H. Dong, J. Bai, Y. Li, S. Li and M. Scheer. *J. Am. Chem. Soc.* 130 (2008) 7778-7779; S. L. Georgopoulos, R. Diniz, M. I. Yoshida, N. L. Speziali, H. F. Dos Santos, G. M. A. Junqueira and L. F. C. de Oliveira, *J. Mol. Struct.* 794 (2006) 63-70.
- [3] R. West and H. Y. Niu, *Inorg. Chem.* 85 (1963) 2589-2590.
- [4] M. Habenschuss and B. C. Gerstein, *J. Chem. Phys.* 61 (1974) 852-860.
- [5] C. Robl and A. Weiss, *Z. Naturforsch.* 41b (1986) 1341-1345.
- [6] H. Kugamai, H. Sobukawa and M. Kurmoo, *J. Mater. Sci.* 43 (2008) 2123-2130.
- [7] B.-P. Yang and J.-G. Mao, *Inorg. Chem.* 44 (2005) 566-571.
- [8] X. Solans, M. Aguiló, A. Gleizes, J. Faus, M. Julve and M. Verdaguer, *Inorg. Chem.* 29 (1990) 775-784 and references cited therein.
- [9] C.-R. Lee, C.-C. Wang and Y. Wang, *Acta Crystallogr. B* 52 (1996) 966-975 and references cited therein.
- [10] D. Dan and C. N. R. Rao, *Solid State Sci.* 5 (2003) 615-620 and references cited therein.
- [11] P. Millet, L. Sabadié, J. Galy and J. C. Trombe, *J. Solid State Chem.* 173 (2003) 49-53.
- [12] W. J. Oldham, B. L. Scott, K. D. Abney, W. H. Smith and D. A. Costa, *Acta Crystallogr. C* 58 (2002) m139-m140.
- [13] J. Fan, M. H. Shu, T. Okamura, Y. Z. Li, W. Z. Sun, W. X. Tang and N. Ueyama, *New J. Chem.* 27 (2003) 1306-1307.
- [14] S. Gao, Z. B. Zhu, L. H. Huo and S. W. Ng, *Acta Crystallogr. E* 61 (2005) m528-m530.
- [15] L. A. Hall, D. J. Williams, S. Menzer and A. J. P. White, *Inorg. Chem.* 36 (1997) 3096-3101.
- [16] R. Köferstein and C. Robl, *Z. Anorg. Allg. Chem.* 629 (2003) 371-373.
- [17] J. P. Auffrédic, J. Plévert, and D. Louër, *J. Solid State Chem.* 84 (1990) 58-70.
- [18] A. Boulitif and D. Louër, *J. Appl. Crystallogr.* 37 (2004) 724-731.
- [19] V. Favre-Nicolin and R. Cerny, *J. Appl. Crystallogr.* 35 (2002) 734-743.
- [20] J. Rodriguez-Carvajal, *Physica B* 192 (1993) 55-69; T. Roisnel and J. Rodriguez-Carvajal, *Mater. Sci. Forum.* 118 (2001) 378-381.
- [21] Nonius, Kappa CCD Program Software, (Nonius BV, Delft, The Netherlands,) (1998).
- [22] Z. Otwinowski and W. Minor, *Methods in Enzymology.* 276 (1997), *Macromolecular Crystallography*, part A, pp. 307-326; ed. C. W. Carter, Jr. and R. M. Sweet, Academic Press.
- [23] J. de Meulenaer and H. Tompa, *Acta Crystallogr.* 19 (1965) 1014-1018.
- [24] M. C. Burla, M. Camalli, B. Carrozzini, G. L. Casciarano, C. Giacovazzo, G. Polidori and R. Spagna, *J. Appl. Crystallogr.* 36 (2003) 1103.
- [25] G. M. Sheldrick, *SHELXL-97: programs for crystal structure refinement*, University of Göttingen, Germany. (1997).
- [26] X. Guan and R. E. Stark, *Solid State Nuc. Mag. Res.* 38 (2010) 74-76
- [27] D. Massiot, F. Fayon, M. Capron, I. King, S. Le Calvé, B. Alonso, J. O. Durand, B. Bujoli, Z. Gan, G. Hoatson, *Magn. Reson. Chem.* 40 (2002) 70-76
- [28] Powder Diffraction File, International Centre for Diffraction Data, Newtown Square, PA, USA.
- [29] D. L. Perry and T. J. Wilkinson, *Appl. Phys. A.* 89 (2007) 77-80.
- [30] T. Bataille, N. Audebrand, A. Boulitif and D. Louër, *Z. Kristallogr.* 219 (2004) 881-891.
- [31] C. A. Sorrell, *J. Am. Ceram. Soc.* 56 (1973) 613-618.
- [32] S. H. Dale, M. R. J. Elsegood and S. Kainth, *Acta Crystallogr. C* 60 (2004) m76-m78.
- [33] H. Furutachi, S. Fujinami and H. Okawa, *J. Chem. Soc. Dalton Trans.* (2000) 2761-2769.
- [34] F. Fayon, I. Farnan, C. Bessada, J. Coutures, D. Massiot, J. P. Coutures, *J. Am. Chem. Soc.* 119 (1997) 6837-6843
- [35] C. Boudaren, J. P. Auffrédic, P Bénard-Rocherullé and D. Louër, *Solid State Sci.* 3 (2001) 847-858.

- [36] K.-L. Zhang, W. Liang, Y. Chang, L.-M. Yuan and S. W. Ng, *Polyhedron* 28 (2009) 647-652.
- [37] N. Mahé and T. Bataille, *Inorg. Chem.* 43 (2004) 8379-8386.
- [38] B. Zheng, J. Bai and Z. Zhang, *CrystEngComm.* 12 (2010) 49-51.
- [39] X. Duan and D. G. Evans, *Structure and Bonding: Layered Double Hydroxides*, Springer-Verlag, Berlin, Heidelberg, 119 (2005).
- [40] C. Robl and A. Weiss, *Z. Anorg. Allg. Chem.* 546 (1987) 161-168.
- [41] M. Lahtinen and J. Valkonen, *Chem. Mater.* 14 (2002) 1812-1817.
- [42] A. M. Arevalo-Lopez and M. A. Alario-Franco, *J. Solid State Chem.* 180 (2007) 3271-3279.

**Table 1.**  
Crystallographic data of reported phases

Compound	Pb(H <sub>2</sub> O)(C <sub>4</sub> O <sub>4</sub> ) (1)	PbC <sub>4</sub> O <sub>4</sub> (2)	PbC <sub>4</sub> O <sub>4</sub> (3)
Empirical formula	C <sub>4</sub> H <sub>2</sub> O <sub>5</sub> Pb	C <sub>4</sub> O <sub>4</sub> Pb	C <sub>4</sub> O <sub>4</sub> Pb
Fw (g mol <sup>-1</sup> )	337.26	319.24	319.24
Space Group	<i>P2<sub>1</sub>/c</i>	<i>Cmma</i>	<i>I4/mcm</i>
method	powder	powder	single-crystal
T (K)	298	413	298
$\lambda$ (Å)	1.5406	1.5406/1.5444	0.71073
<i>a</i> (Å)	7.36353(8)	24.276(6)	6.1640(2)
<i>b</i> (Å)	11.3014(1)	15.261(3)	6.1640(2)
<i>c</i> (Å)	6.68066(8)	7.851(2)	12.0526(8)
$\alpha$ (°)	90	90	90
$\beta$ (°)	102.4985(7)	90	90
$\gamma$ (°)	90	90	90
<i>V</i> (Å <sup>3</sup> )	542.78(1)	2908.4	457.94(4)
<i>Z</i>	4	—	4
Crystal dim (mm <sup>3</sup> )	—	—	0.112x0.091x0.043
$\rho_{\text{calc}}$ (g cm <sup>-3</sup> )	4.13	—	4.63
2 $\theta$ range (°)	10-130	5-120	5.82-54.97
No of reflections	934	1163	2197
indep reflns [ <i>I</i> > 2 $\sigma$ ( <i>I</i> )]	—	—	142
No param / restraints	67 / 0	—	15 / 0
R <sub>B</sub>	0.0358	—	—
R <sub>F</sub> / R <sub>1</sub>	0.0234	—	0.0281
R <sub>p</sub>	0.0813	—	—
R <sub>wp</sub> / wR <sub>2</sub>	0.109	—	0.0774 <sup>s</sup>
X <sup>2</sup> / GooF	1.62	—	1.238

$$^s w = 1/[\sigma^2(F_o^2) + (0.0450P)^2 + 0.6085P] \text{ where } P = (F_o^2 + 2F_c^2)/3$$

**Table 2.**

Atomic coordinates and isotropic atomic displacement parameters

Atom	x/a	y/b	z/c	$U_{eq}$
Pb(H <sub>2</sub> O)(C <sub>4</sub> O <sub>4</sub> ) (1)				
Pb	0.2675(1)	0.40903(9)	0.6127(2)	0.0072(6)
Ow	0.460(2)	0.056(1)	0.785(2)	0.002(4)
O1	0.119(2)	0.895(1)	0.968(2)	0.005(2)
O2	-0.124(2)	0.700(1)	0.764(2)	0.005(2)
O3	0.202(2)	0.502(1)	0.940(2)	0.005(2)
O4	0.467(2)	0.721(1)	0.141(2)	0.005(2)
C1	0.155(3)	0.796(2)	0.972(3)	0.001(3)
C2	0.036(3)	0.698(2)	0.870(3)	0.001(3)
C3	0.185(3)	0.613(2)	0.942(3)	0.001(3)
C4	0.296(3)	0.708(2)	0.031(3)	0.001(3)
PbC <sub>4</sub> O <sub>4</sub> (2)				
Pb1	0.4059(4)	1/4	0.177(1)	
Pb2	0.9108(4)	0	1/2	
Pb3	0.1625(4)	1/2	0	
PbC <sub>4</sub> O <sub>4</sub> (3)				
Pb	0	0	1/4	0.0143(4)
O	0.3154(4)	0.1846(4)	0.1354(3)	0.0187(9)
C	0.4158(6)	0.0842(6)	0.0605(5)	0.012(1)

**Table 3.**  
Selected bond distances (Å)

Pb–O pairs		closest Pb···Pb pairs	
Pb(H <sub>2</sub> O)(C <sub>4</sub> O <sub>4</sub> ) (1)			
Pb–O1	2.56(1) / 2.79(1)	Pb···Pb	4.41 / 4.52 / 4.91
Pb–O2	2.79(1) / 2.80(1)		
Pb–O3	2.56(1)		
Pb–O4	2.70(1)		
Pb–Ow	2.58(1) / 2.88(1)		
PbC <sub>4</sub> O <sub>4</sub> (2)			
		Pb1···Pb1	4.43
		Pb1···Pb2	4.54
		Pb1···Pb3	4.41
		Pb2···Pb2	4.02
		Pb2···Pb3	4.34
		Pb3···Pb3	4.42
PbC <sub>4</sub> O <sub>4</sub> (3)			
Pb–O	2.643(2)	Pb···Pb	4.36

## Figure captions

Figure 1. Temperature Dependent X-ray Powder Diffraction patterns for the thermal decomposition of lead squarate tetrahydrate (air flux, 10 C h<sup>-1</sup>, 1800 s per pattern).

Figure 2. TG analysis of lead squarate monohydrate (air flux, 10 C h<sup>-1</sup>).

Figure 3. Rietveld refinement plot for Pb(H<sub>2</sub>O)(C<sub>4</sub>O<sub>4</sub>) (**1**) showing experimental data (dots), the calculated pattern (full line) and the difference curve. The Bragg peaks of the principal phase are given at the upper line, the lower bars corresponding to those of PbC<sub>4</sub>O<sub>4</sub> (**3**). The plot is magnified (x 16.5) in the high angle region.

Figure 4. Powder diffraction patterns of (a) Pb(H<sub>2</sub>O)(C<sub>4</sub>O<sub>4</sub>) (**1**), containing a tiny amount of PbC<sub>4</sub>O<sub>4</sub> (**3**), for which the powder pattern (b) is calculated from single-crystal data; (c) PbC<sub>4</sub>O<sub>4</sub> (**2**), obtained after heating the precursor at ca 30 °C h<sup>-1</sup>, which contains a significant quantity of (**3**) (+); (d) PbC<sub>4</sub>O<sub>4</sub> (**2**) after gentle heating, which contains a small amount of monohydrate (**1**) (\*) and a few of polymorph (**3**) (+).

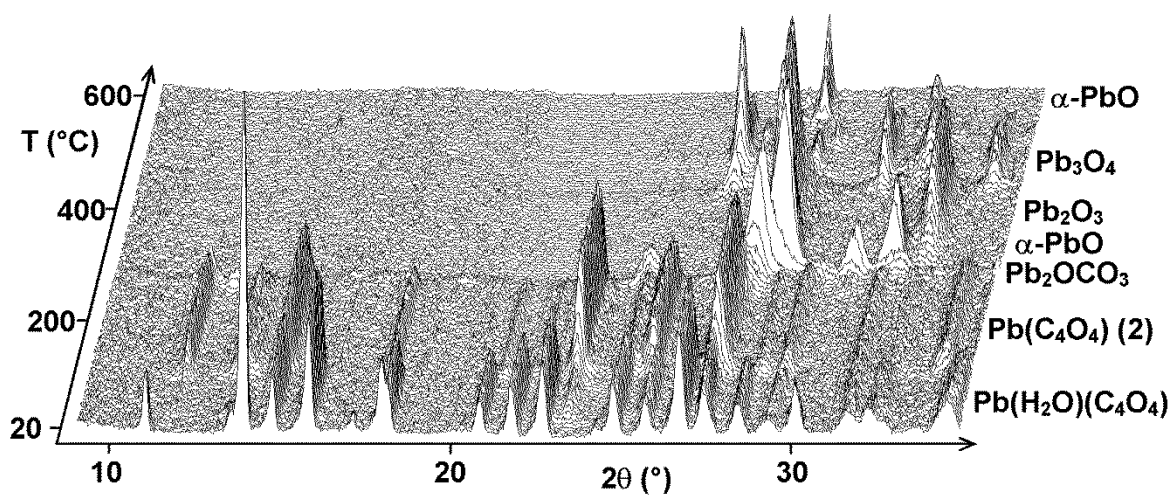
Figure 5. (a) A part of the structure of Pb(H<sub>2</sub>O)(C<sub>4</sub>O<sub>4</sub>) (**1**) showing the asymmetric unit and the environment of both Pb and C<sub>4</sub>O<sub>4</sub>; (b) the connectivity of Pb polyhedra, chains are represented by alternate colors.

Figure 6. (a) Focus on the isotropic part of experimental <sup>1</sup>H MAS NMR spectrum, total fit and fit components, at a spinning rate of 14 kHz. The four components of the fit are denoted H<sub>1</sub>, H<sub>2</sub>, H<sub>3</sub> and H<sub>4</sub> and correspond to isotropic chemical shifts of 1.75, 4.56, 6.53, and 9.10 ppm, with integrated intensities of 8%, 22%, 37% and 33% respectively; (b) Focus on the isotropic part of experimental <sup>207</sup>Pb MAS NMR spectrum, total fit and fit components, at a spinning rate of 13.3 kHz. The two components of the fit are denoted Pb<sub>1</sub> and Pb<sub>2</sub>, and correspond to isotropic chemical shifts of -2401 and 2417 ppm, with integrated intensities of 30% and 70% respectively.

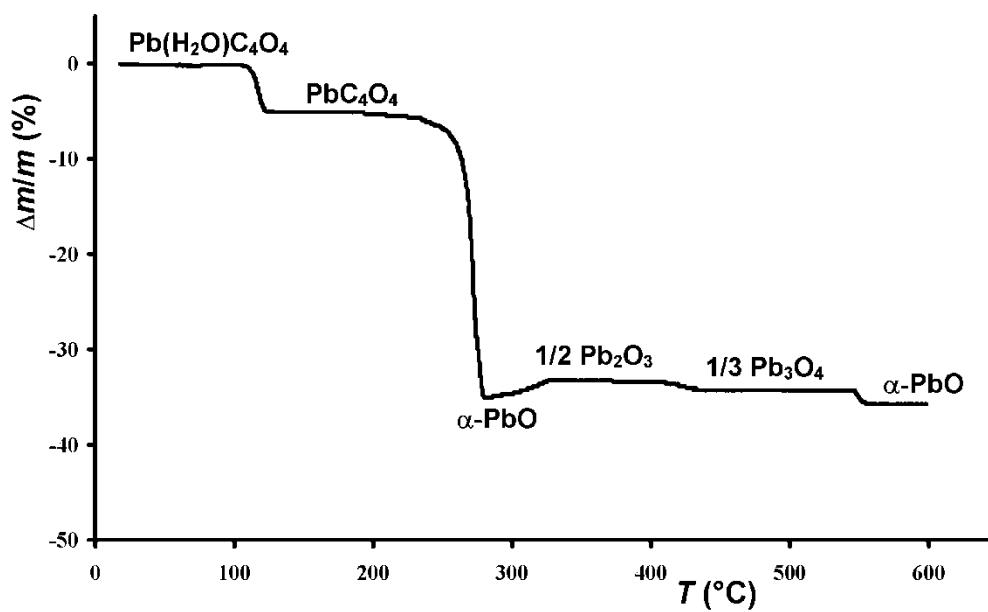
Figure 7. Partial structure of PbC<sub>4</sub>O<sub>4</sub> (**2**) showing the Pb network.

Figure 8. Pillared structure of PbC<sub>4</sub>O<sub>4</sub> (**3**).

Figure 9. Simplified representation of the Pb environment and the structural arrangement of the all phases obtained during dehydration of (a) Pb(H<sub>2</sub>O)<sub>4</sub>(C<sub>4</sub>O<sub>4</sub>), i.e., (b) Pb(H<sub>2</sub>O)(C<sub>4</sub>O<sub>4</sub>) (**1**), (c) PbC<sub>4</sub>O<sub>4</sub> (**3**) and (d) PbC<sub>4</sub>O<sub>4</sub> (**2**). The closest Pb···Pb distances are represented as orange lines and blue bonds are given for water molecules.



**Fig.1.** Temperature Dependent X-ray Powder Diffraction patterns for the thermal decomposition of lead squarate tetrahydrate (air flux,  $10\text{ C h}^{-1}$ , 1800 s per pattern)



**Fig.2.** TG analysis of lead squarate monohydrate (air flux,  $10 \text{ C h}^{-1}$ )

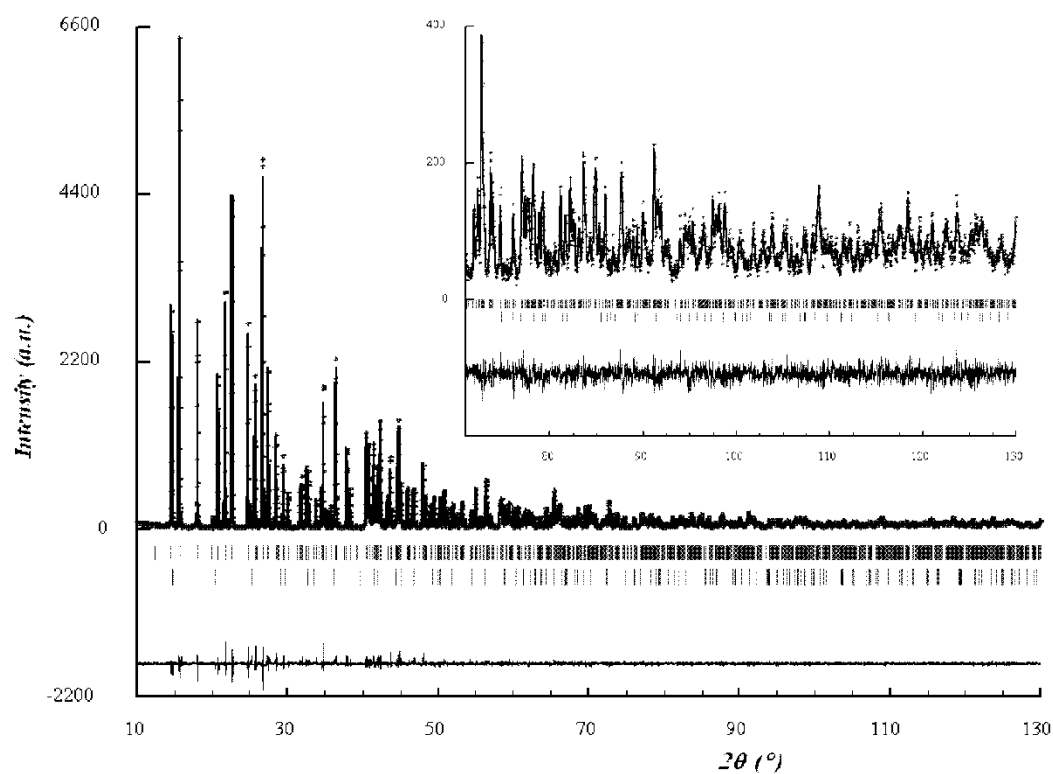


**Fig.3.** Rietveld refinement plot for  $\text{Pb}(\text{H}_2\text{O})(\text{C}_4\text{O}_4)$  (**1**) showing experimental data (dots), the calculated pattern (full line) and the difference curve. The Bragg peaks of the principal phase are given at the upper line, the lower bars corresponding to those of  $\text{PbC}_4\text{O}_4$  (**3**). The plot is magnified ( $\times 16.5$ ) in the high angle region.

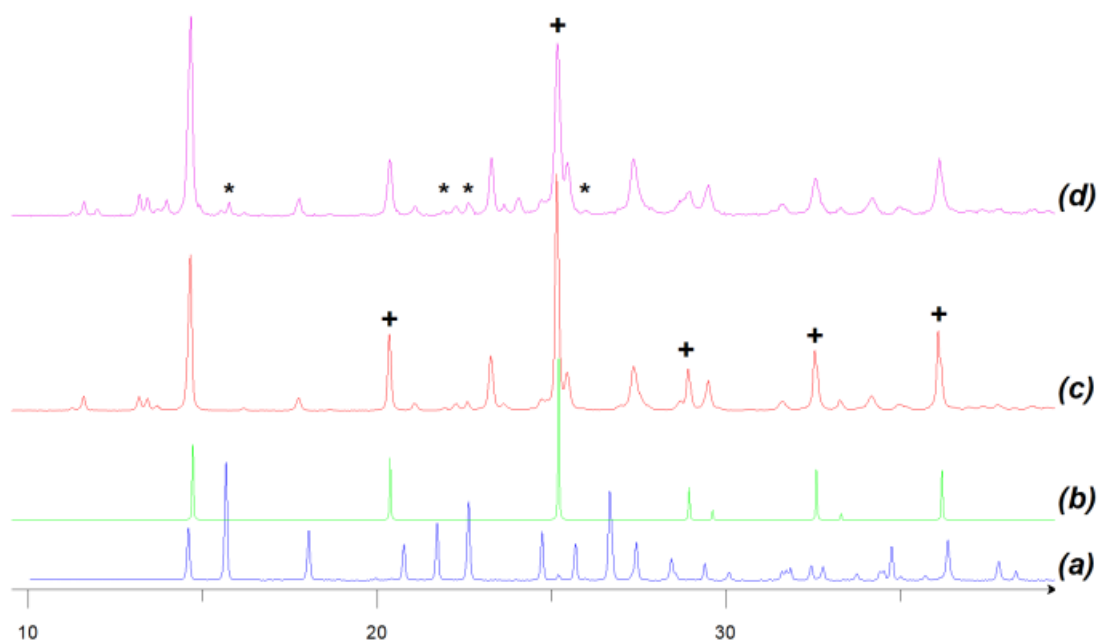


**Fig.4.** Powder diffraction patterns of (a)  $\text{Pb}(\text{H}_2\text{O})(\text{C}_4\text{O}_4)$  (1), containing a tiny amount of  $\text{PbC}_4\text{O}_4$  (3), for which the powder pattern (b) is calculated from single-crystal data; (c)  $\text{PbC}_4\text{O}_4$  (2), obtained after heating the precursor at ca  $30\text{ }^\circ\text{C h}^{-1}$ , which contains a significant quantity of (3) (+); (d)  $\text{PbC}_4\text{O}_4$  (2) after gentle heating, which contains a small amount of monohydrate (1) (\*) and a few of polymorph (3) (+).

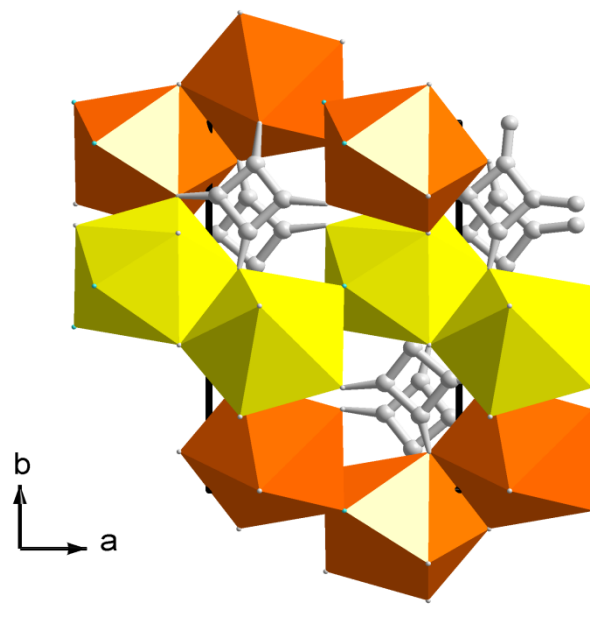
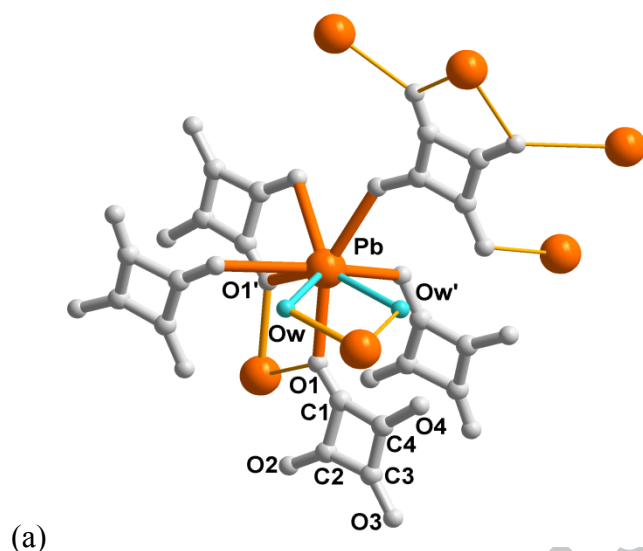


**Fig.5.** (a) A part of the structure of  $\text{Pb}(\text{H}_2\text{O})(\text{C}_4\text{O}_4)$  (**1**) showing the asymmetric unit and the environment of both Pb and  $\text{C}_4\text{O}_4$ ; (b) the connectivity of Pb polyhedra, chains are represented by alternate colors.

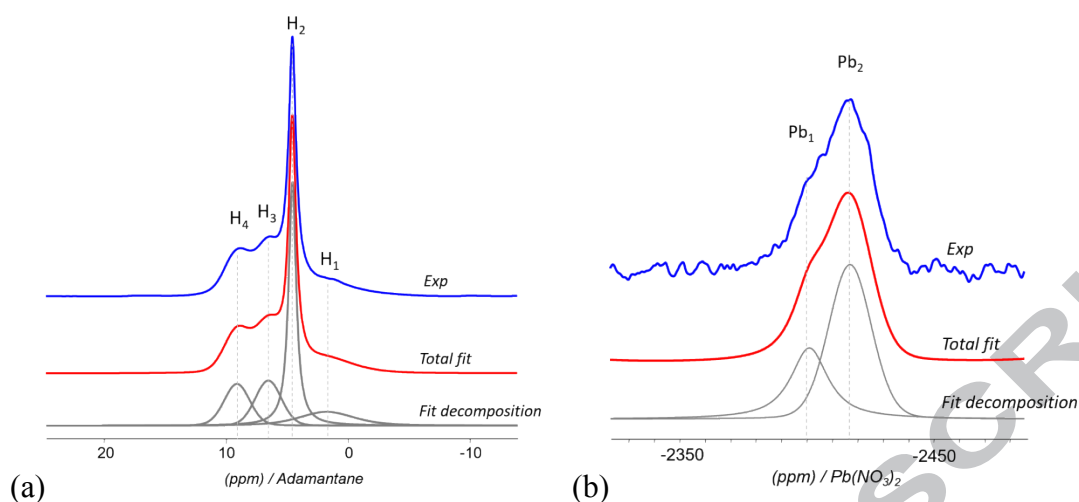


**Fig.6.** (a) Focus on the isotropic part of experimental  $^1\text{H}$  MAS NMR spectrum, total fit and fit components, at a spinning rate of 14 kHz. The four components of the fit are denoted  $\text{H}_1$ ,  $\text{H}_2$ ,  $\text{H}_3$  and  $\text{H}_4$  and correspond to isotropic chemical shifts of 1.75, 4.56, 6.53, and 9.10 ppm, with integrated intensities of 8%, 22%, 37% and 33% respectively; (b) Focus on the isotropic part of experimental  $^{207}\text{Pb}$  MAS NMR spectrum, total fit and fit components, at a spinning rate of 13.3 kHz. The two components of the fit are denoted  $\text{Pb}_1$  and  $\text{Pb}_2$ , and correspond to isotropic chemical shifts of -2401 and 2417 ppm, with integrated intensities of 30% and 70% respectively.

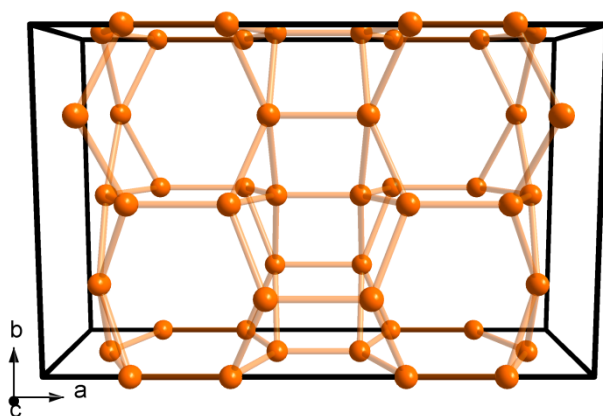


**Fig.7.** Partial structure of  $\text{PbC}_4\text{O}_4$  (2) showing the Pb network.

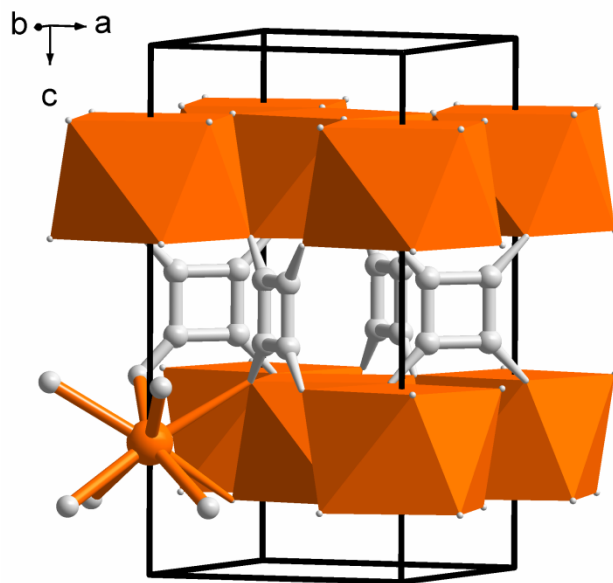


**Fig.8.** Pillared structure of  $\text{PbC}_4\text{O}_4$  (3).

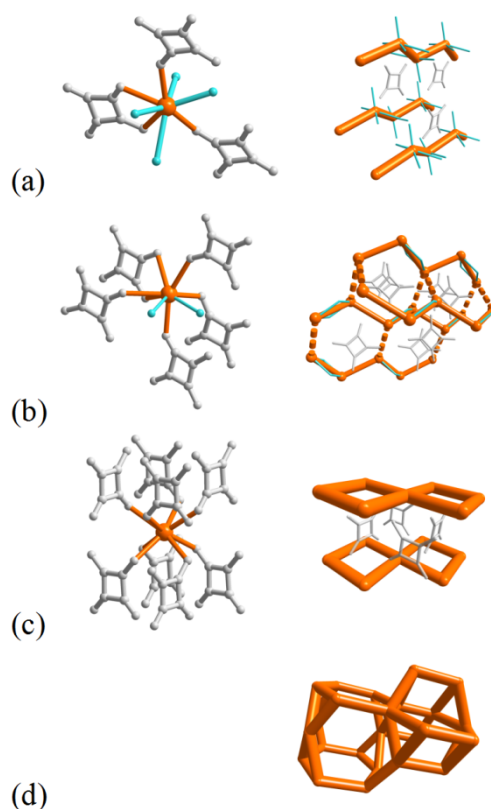
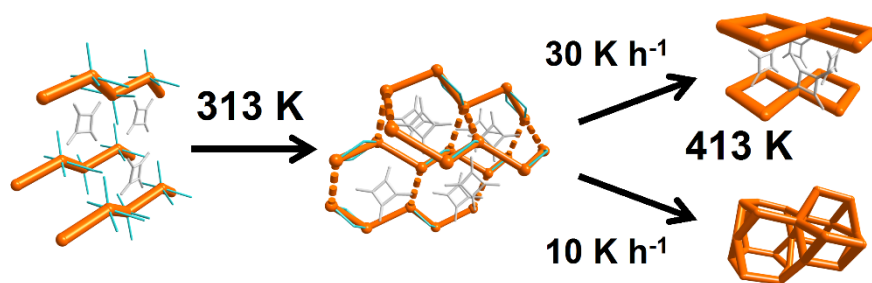


**Fig.9.** Simplified representation of the Pb environment and the structural arrangement of the all phases obtained during dehydration of (a)  $\text{Pb}(\text{H}_2\text{O})_4(\text{C}_4\text{O}_4)$ , i.e., (b)  $\text{Pb}(\text{H}_2\text{O})(\text{C}_4\text{O}_4)$  (**1**), c)  $\text{PbC}_4\text{O}_4$  (**3**) and d)  $\text{PbC}_4\text{O}_4$  (**2**). The closest  $\text{Pb}\cdots\text{Pb}$  distances are represented as orange lines and blue bonds are given for water molecules.

The condensation of the crystal structure of lead squarate tetrahydrate subjected to dehydration is fully described. Depending on how fast the last water molecule is released, two polymorphs of lead squarate are obtained.



ACCEPTED

